

1 **On the multifractal features of low-frequency magnetic field**
2 **fluctuations in the field-aligned current ionospheric polar**
3 **regions: Swarm observations**

4 **G. Consolini¹, P. De Michelis², T. Alberti¹, F. Giannattasio², I. Coco², R. Tozzi², and T. T. S.**
5 **Chang³**

6 ¹INAF-Istituto di Astrofisica e Planetologia Spaziali, 00133 Rome, Italy

7 ²Istituto Nazionale di Geofisica e Vulcanologia, 00143 Rome, Italy

8 ³Kavli Institute for Astrophysics and Space Research, Massachusetts Institute of Technology, Cambridge, MA 02139 USA

9 **Key Points:**

- 10 • Low frequency magnetic field fluctuations in the topside F-region polar ionosphere:
11 evidence for scale-invariance.
- 12 • Anomalous scaling (multifractal/intermittent) features and anisotropy of magnetic
13 field fluctuations.
- 14 • Link between the scale-invariant nature of fluctuations and the filamentary character
15 of field-aligned currents.

Corresponding author: Giuseppe Consolini, giuseppe.consolini@inaf.it

Abstract

Recent findings on the nature of magnetic field fluctuations in the high-latitude ionospheric regions have suggested the existence of scaling features, which are the signature of the occurrence of turbulence. These features mainly characterize the magnetic field fluctuations in those regions where the field-aligned currents flow. Here, we investigate the nature of the Earth's magnetic field fluctuations using the high-resolution (50 Hz) magnetic measurements from the ESA Earth's observation mission Swarm. Our study indicates that spatio-temporal anomalous scaling features characterize low frequency magnetic field fluctuations in the high-latitude ionospheric regions of field-aligned currents at spatial scales in the range [0.8, 80] km (timescales in the range [0.1, 10] s). The signature of a multifractal nature of these fluctuations suggests a highly complex structure of the field-aligned currents. Our results support the view of inhomogeneous (filamentary) field-aligned currents, which can have relevant implications in the comprehension of the physical processes responsible for the magnetospheric-ionospheric coupling and ionospheric heating.

1 Introduction

Since the early 90s it has been argued that several regions of the circumterrestrial space are characterized by a multiscale dynamics, which is mainly due to the occurrence of intermittent turbulent phenomena and complexity [Borovsky *et al.*, 1997; Chang *et al.*, 2003, 2004; Bruno & Carbone, 2016]. Indeed, turbulence, which is a prevalent phenomenon in space plasmas, generates multiscale coherent structures over a wide range of spatio-temporal scales. In magnetized plasmas these coherent structures, consisting of bundles of fluctuations, may take the shape of flux tubes, current filaments, propagating nonlinear solitary waves, convective structures and so on, depending on the local and global magnetic field and plasma topology [Chang *et al.*, 2004]. In the near-Earth central plasma sheet of the magnetospheric tail region, the stochastic evolution and interaction of such coherent structures are suggested to be responsible for the occurrence of sporadic plasma acceleration, heating and energization (e.g., bursty bulk flows, localized reconnections). These processes have been detected by several space missions, such as ISEE, AMPTE, Cluster [Lui *et al.*, 1998; Angelopoulos *et al.*, 1999; Chang *et al.*, 2003, 2004], and have been suggested to be responsible for the stochastic nature of auroral breakups [Lui *et al.*, 1998]. A further consequence of the dynamics of such coherent structures is the emergence of spatio-temporal intermittency in an overall turbulent plasma, i.e., an inhomogeneous turbulent energy dissipation pattern.

In the framework of high-latitude ionosphere, turbulence is expected to be a relevant phenomenon in the polar regions where particle precipitation occurs [Kintner and Seyler, 1985]. Indeed, in some cases turbulence has been invoked to explain the formation of ionospheric irregularities [Booker, 1956; Dagg, 1957; Kintner and Seyler, 1985]. According to Kintner and Seyler [1985] the range of scales where turbulence plays a relevant role, is from few meters up to ~ 1000 km in the topside F-region of the high-latitude ionosphere, a range of spatial scales where large magnetic and electric field fluctuations have been observed. In recent years, an extensive literature has demonstrated that high-latitude magnetic and electric field fluctuations, as well as, plasma density variations, show scale-invariance and intermittent turbulent features [Tam *et al.*, 2005; Golovchanskaya *et al.*, 2006; Spicher *et al.*, 2015; De Michelis *et al.*, 2015, 2017]. Furthermore, the scale-invariance nature of magnetic field fluctuations has been shown to be a function of the different polar regions (polar cap, cusp, auroral oval), the magnetic local time, the interplanetary magnetic field conditions and the geomagnetic activity disturbance level [De Michelis *et al.*, 2015, 2017, 2019].

Different mechanisms have been proposed as possible sources of the observed turbulent fluctuations, among which the occurrence of strong shear flows and particle precipitations seems to play a relevant role. Thus, among the different high-latitude ionospheric

67 regions (i.e., polar cap, cusp, auroral oval, etc.), those associated with the field-aligned
 68 currents with particle precipitation enhancements during periods of high geomagnetic ac-
 69 tivity represent a good candidate for turbulence to occur. This scenario is supported by the
 70 experimental work of *Pokhotelov et al.* [1994] where it has been shown that a likely phys-
 71 ical mechanism for the excitation of turbulent noise fluctuations in the ionospheric plasma
 72 can be the occurrence of localized field-aligned currents and the related current instabili-
 73 ties.

74 The field-aligned currents (FACs) were originally postulated by Birkeland [*Birke-*
 75 *land*, 1908] and detected for the first time sixty years later by spacecraft observations of
 76 localized magnetic fluctuations [*Zmuda et al.*, 1966; *Cummings and Dessler*, 1967]. One
 77 of the first sketch of these electric currents was proposed by *Iijima and Potemra* [1976,
 78 1978] based upon the analysis of the single-polar-orbiting Triad satellite. In this sketch,
 79 the pattern of the distribution of FACs, also known as Birkeland currents, is represented
 80 by two belts of electric currents (region-1 and region-2) that flow upward and downward
 81 along the magnetic field lines according to the latitude and magnetic local time. Later, by
 82 analyzing the periods characterised by a northward interplanetary magnetic field, *Iijima*
 83 [1984] and *Iijima and Shibaji* [1987] found another stable FAC system at higher latitude
 84 than region-1, the so-called Northward B_Z FAC system. FACs are located at high-latitudes
 85 in both hemispheres, and flow along geomagnetic field lines connecting the Earth's mag-
 86 netosphere to the ionosphere and playing an important role in energy and momentum
 87 transfer between different plasma regions: the solar wind and magnetosphere on the one
 88 hand and the ionosphere and thermosphere on the other hand. As a consequence, the
 89 knowledge of their structure and dynamics is of uppermost importance to the understand-
 90 ing how the solar wind energy is transferred from the magnetosphere to the ionosphere
 91 and thermosphere and to the comprehension of those physical processes which are related
 92 to the solar wind-magnetosphere-ionosphere coupling.

93 In recent years, there has been an increasing amount of literature on the statistical
 94 investigation of high latitude FACs using observations mainly from low-orbiting satellites
 95 (e.g., CHAMP, AMPERE, DMSP and Swarm). Results have been also compared with
 96 studies on the large scale convection topology based on ground-based magnetometer net-
 97 works and coherent/incoherent auroral radars (e.g., EISCAT and SuperDARN) [*Sofko et*
 98 *al.*, 1995; *Chisham et al.*, 2007]. The morphology of this current system on large spa-
 99 tial scales is now well established [*Anderson et al.*, 2008; *Gjerloev et al.*, 2011], as well
 100 as, its variability with solar wind-magnetosphere coupling conditions [*Anderson et al.*,
 101 2005; *Korth et al.*, 2010; *Cheng et al.*, 2013] and its dynamics with respect to various
 102 geophysical, seasonal and local time conditions [*Papitshvili et al.*, 2001; *Christiansen et*
 103 *al.*, 2002; *Papitashvili et al.*, 2002]. Although significant progresses have been achieved
 104 on this three-dimensional current flow in the auroral zone, some scientific questions re-
 105 main to be answered. In this context, an interesting topic is the characterization of the
 106 field-aligned current structure on small spatial scales. Indeed, in addition to large-scale
 107 FAC structures, which are characterized by widths from few hundreds to a thousand kilo-
 108 meters, some small-scale FAC structures were also observed by satellite measurements
 109 [*Lühr et al.*, 1994; *Stasiewicz and Potemra*, 1998; *Neubert and Christiansen*, 2003]. Sur-
 110 veys such as those conducted by *Neubert and Christiansen* [2003] have shown that small-
 111 scale field-aligned currents can be found throughout the auroral oval although the most
 112 intense of these are in the cusp and pre-noon cusp region. These currents, with typical
 113 widths of a few hundred meters, have intensities reaching several hundreds μAm^{-2} [*Lühr*
 114 *et al.*, 1994; *Stasiewicz and Potemra*, 1998]. It has been also suggested that the small-scale
 115 field-aligned currents can have an important role in the heating of ionosphere and ther-
 116 mosphere. For this reason it is not enough to consider only the FAC structures on large
 117 scales but also important to take into account the local heating resulting from FAC struc-
 118 tures on small scales [*Neubert and Christiansen*, 2003], whose intensity is several orders
 119 of magnitude larger than those characterizing the FAC structures on large scales. It is ex-
 120 pected that the heating of the ionosphere and thermosphere due to the processes related

121 to FACs can be larger when FACs at all scales are considered. For this reason it is impor-
 122 tant to characterize them and investigate their energy deposition at all scales in the future
 123 comprehensive models of magnetosphere-ionosphere-thermosphere coupling.

124 It has been argued that small-scale FACs are probably randomly oriented due to
 125 their possible filamentary structure, while the FACs on the large-scale tend to be organized
 126 in sheets. These sheets tend to break up into individual filaments due to the development
 127 of multiscale magnetic structures in the form of flux tubes and consequently to the devel-
 128 opment of turbulence. These structures are somewhat similar to those found, for example,
 129 in a fluid flow with adjacent layers of different velocities when the Kelvin-Helmholtz in-
 130 stability develops [see, e.g., *Keller et al.*, 1999, and references]

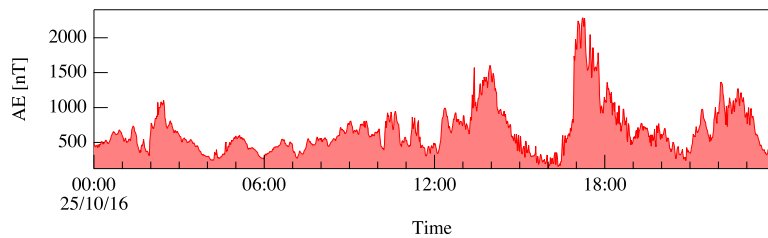
131 The aim of this work is to analyze the turbulent and intermittent nature of small-
 132 scale spatio-temporal magnetic field fluctuations in the high-latitude ionospheric regions
 133 where FACs flow, as a function of the geomagnetic activity disturbance level, and to dis-
 134 cuss the relevance of the observed features with respect to an inhomogeneous structure
 135 of these currents. In the Earth's ionosphere the turbulence may, indeed, be able to gener-
 136 ate/create magnetic and plasma structures that can strongly affect plasma homogeneity
 137 thus playing a relevant role in the FACs topology.

138 2 Data and processing approach

139 This study is based on *in-situ* magnetic field observations from one of the three
 140 Swarm satellites, Swarm A.

141 The Swarm constellation consists of three identical satellites, which fly in two dif-
 142 ferent orbital planes at two different altitudes. Two satellites (Swarm A and Swarm C)
 143 fly side-by-side at a mean altitude of approximately 460 km in a plane of 87.4° inclina-
 144 tion during the considered time interval. The third satellite (Swarm B) orbits at a higher
 145 altitude than the others, flying about 50 km above in a plane of 88° inclination [*Friis-*
 146 *Christensen et al.*, 2006]. Each satellite is equipped with identical instruments: an absolute
 147 scalar magnetometer (ASM), a vector field magnetometer (VFM), an accelerometer (ACC)
 148 and an Electric Field Instrument (EFI) comprising of two Thermal Ion Imagers (TIIs) and
 149 two Langmuir probes (LPs) [*Knudsen et al.*, 2017].

150 Being interested in the analysis of the properties of the low frequency magnetic
 151 field fluctuations in the regions of FACs, we select a day characterized by a mid-high ge-
 152 omagnetic activity level according to the Auroral Electroject (AE) index. The selected
 153 day is October 25th, 2016, during which the AE index ranges from 125 nT to ~ 2300 nT
 154 ($\langle \text{AE} \rangle \sim 660$ nT) (see Figure 1). This day is characterized by quite variable interplanetary
 155 conditions with a B_Z^{GSM} mainly negative ($\langle B_Z^{GSM} \rangle = -2.2$ nT), a solar wind speed that
 156 increases from ~ 400 km (slow solar wind) in the first half of the day, to ~ 700 km (fast
 157 solar wind) in the second half of the day. Differently, low latitudes are characterized by a
 158 low geomagnetic activity ($SYM - H \in [-81, -21]$ nT).



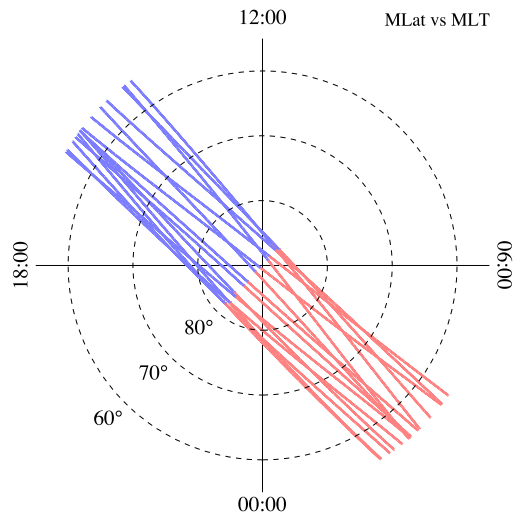
159 **Figure 1.** AE index values (1-minute time resolution) during October 25th, 2016.

160 For this day we consider the Level 1b high-resolution (50 Hz) magnetic field data
 161 along the three magnetic components (X, Y and Z in the North-East-Center frame of ref-
 162 erence) sampled by the fluxgate magnetometer on-board of Swarm A. We use the
 163 *SW_OPER_MAGA_HR_IB* file type according to ESA nomenclature, which are available
 164 at <ftp://swarm-diss.eo.esa.int>.

165 To be able to investigate, separately, the properties of the magnetic fields generated
 166 in the Northern polar region by the horizontal and field-aligned currents we evaluate the
 167 components parallel and perpendicular to the direction of the main magnetic field of exter-
 168 nal, i.e., magnetospheric and ionospheric, origin. Indeed, the field-aligned currents (Birke-
 169 land currents) are expected to produce a magnetic field perturbation which is perpendic-
 170 ular to the main geomagnetic field while the currents flowing horizontally in the E-layer
 171 of the ionosphere (auroral electrojets) generate a magnetic field perturbation which are ob-
 172 served along the geomagnetic field lines (i.e., they produce vertical perturbations) near the
 173 current edges [Olsen, 1996]. It follows the need to rotate measurements to a new frame
 174 with axes parallel and perpendicular to the main field. In detail, the parallel component
 175 ($b_{||}$) is locally nearly-coincident with the Z component, while the two perpendicular ones
 176 are almost along the X ($b_{\perp,1}$) and Y ($b_{\perp,2}$) components.

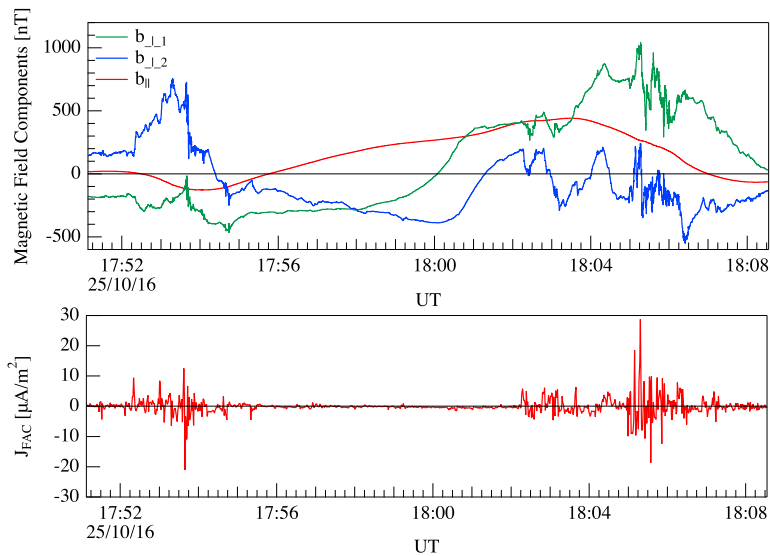
177 Operationally, we remove the contributions coming from the core and crust, as mod-
 178 eled by CHAOS-6 [Finlay, 2015], from the Earth's magnetic field observed onboard Swarm
 179 A. In this way, we are able to exploit the contribution to the geomagnetic field due to
 180 sources located in the ionosphere and magnetosphere only. The obtained residuals in the
 181 North-East-Center (NEC) frame of reference are successively rotated into the new frame
 182 and the components parallel and perpendicular to the direction of the main field evaluated.

183 Figure 2 shows a polar view map in magnetic local time (MLT) and quasi-dipole
 184 magnetic latitude (MLat) of the polar crossings of Swarm A satellite in the Northern
 185 Hemisphere during the selected day (October 25th, 2016). The two colors identify the
 186 crossings in the dayside (blue) and nightside (red), respectively.



187 **Figure 2.** Polar crossings of the Swarm A satellite in the Northern Hemisphere during October 25th, 2016.
 188 The polar view map is in magnetic local time (MLT) and quasi-dipole magnetic latitude (MLat) in the range
 189 from 55° N to 90° N. The colors identify the crossings in the dayside (blue) and nightside (red), respectively.
 190 Dashed circles are drawn at magnetic latitudes of 60°, 70°, and 80°.

191 Figure 3 displays, in the top panel, an example of the magnetic field of external ori-
 192 gin along the components perpendicular and parallel to the main field, estimated for one
 193 crossing over the Northern Hemisphere. In the bottom panel of the same figure, the field-
 194 aligned current density is reported for the same interval. The reported field-aligned cur-
 195 rent density is a Swarm Level-2 (L2-FAC) single-spacecraft product [Ritter *et al.*, 2013]
 196 obtained by considering the Swarm A satellite. It is calculated from the spatial gradi-
 197 ents of the magnetic field observed along the direction defined by the spacecraft orbit
 198 track [Ritter *et al.*, 2013] and it is automatically estimated and available at *ftp://swarm-*
 199 *diss.eo.esa.int (FACATMS_2F file type)*. The knowledge of the position of the field-aligned
 200 currents during the crossings of the Northern high-latitude regions by Swarm A satellite
 201 allows the extraction from the broad dataset of the parallel and perpendicular magnetic
 202 field perturbations for October 25th, which are associated with FAC regions.

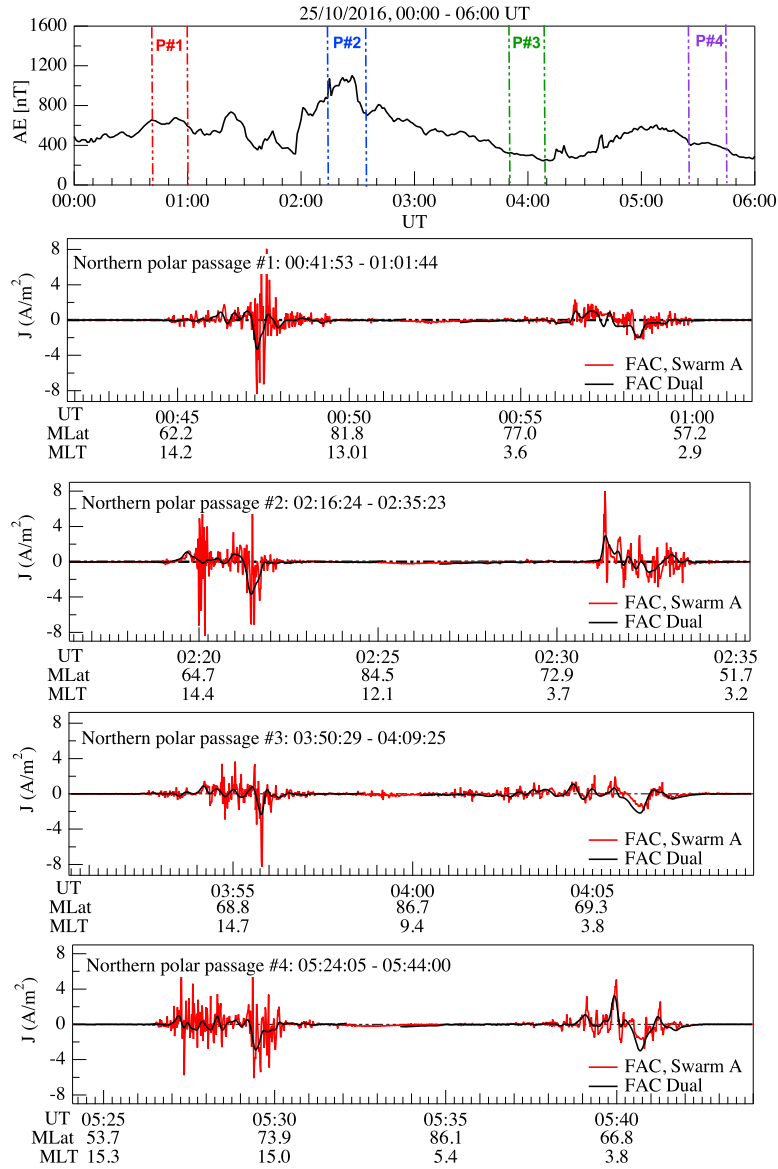


203 **Figure 3.** Top panel: an example of the magnetic field of external origin along the perpendicular and par-
 204 allel components to the main field along a single crossing of the Northern polar region. Bottom panel: the
 205 density of the field-aligned currents obtained as product of Level-2 (L2-FAC) from the data collected by the
 206 Swarm A satellite.

207 Recently, Lühr *et al.* [2016] showed that some FACs structures can be missed using
 208 the single-spacecraft magnetic field measurements and that the dual-satellite approach is
 209 capable of detecting some of these missed structures, thus improving the FAC observa-
 210 tions. However, according to Lühr *et al.* [2016], most of the events missed by the single-
 211 spacecraft technique appear on the nightside and poleward of the auroral oval. Thus, to
 212 check that the selected intervals correctly identify the FAC regions, we also consider the
 213 dual-spacecraft FACs estimate from the pair Swarm A/C during all the crossings of the
 214 high-latitude regions.

215 Figure 4 displays the comparison between the two Level-2 FAC data (single- and
 216 dual-satellite FACs) for the first four of the fifteen crossings of the Northern high-latitude
 217 regions occurred on October 25th, 2016. No discrepancies are observed between the posi-
 218 tion of FACs obtained by the two different techniques. Although FACs are characterized
 219 by different amplitudes, both products locate FACs in the same spatial regions.

220 In practice, to limit our analysis to the regions where the FACs flow, we select only
 221 those time intervals where the local (time-window of 10 s) standard deviation σ_{std} of the
 222 single-spacecraft current (product L2-FAC for Swarm A) is $> 0.03 \text{ A/m}^2$. The value of
 223 $\sigma_{std} \sim 0.03 \text{ A/m}^2$ is the optimal value obtained by a statistical analysis over the entire
 224 considered dataset, that better identifies the border of the FAC regions. The analysis of the
 225 nature of the fluctuations of the magnetic field residuals will be made only for these time
 226 intervals.



227 **Figure 4.** Comparison between the two Level-2 FAC data (single- and dual-satellite FACs) for the first four
 228 of the fifteen crossings of the Northern high-latitude regions occurred on October 25th, 2016. The top panel
 229 shows the first four selected crossings (P#1, P#2, P#3 and P#4 reported in the four successive panels) and the
 230 corresponding values of the AE-index.

3 Analysis and Results

To study the nature of the small-scale low frequency magnetic field fluctuations we perform the analysis of the selected dataset in the temporal domain and evaluate the spectral and scaling features of these small-scale magnetic field fluctuations. This means that we investigate: the power spectral densities (PSDs), the structure functions ($S_q(\tau)$) and the relative scaling of the scaling exponents ($\xi(q)$) as a function of the moment order (q) for the external magnetic field components, perpendicular and parallel to the main field [N.B.: As it will be demonstrated in more detail in the next section, the spacecraft observed low frequency temporal magnetic field fluctuations are dominated primarily by the Doppler-shifted and essentially stationary spatial variations of the field-aligned filamentary current structures. Thus, the time scale τ and frequency f discussed in this section may be viewed essentially as spatial scale $\delta \sim v_{sp}\tau$ and mode number $k \sim 2\pi f/v_{sp}$ with v_{sp} being the spacecraft velocity].

To begin we investigate the average PSDs of the fluctuations of the magnetic field residuals. The PSD would provide us information on the existence of a possible inertial/scaling range which should manifest in a power-law behavior of PSD over a wide range of scales [Kolmogorov, 1941a,b; Frisch, 1995; Biskamp, 2003].

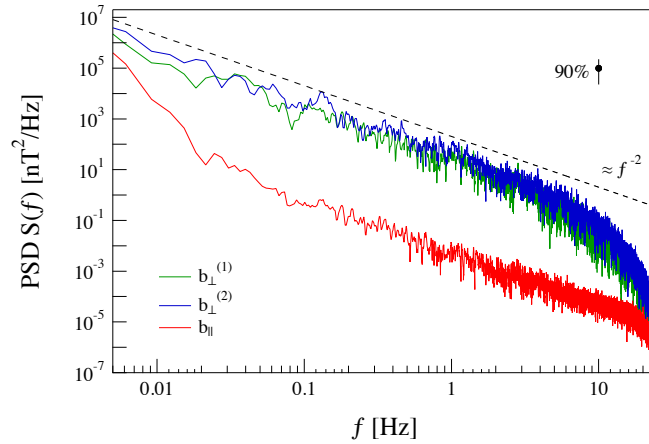
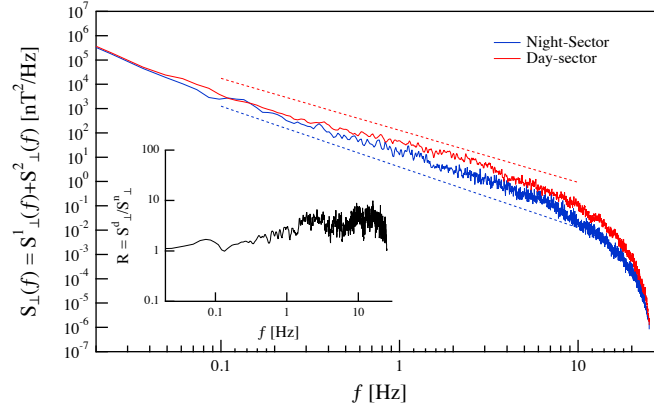


Figure 5. The PSDs of the magnetic field fluctuations along the three directions: two perpendicular and one parallel to the main field. PSDs are reported as a function of frequency and display a power-law decay over about three decades. The dashed line is a power-law dependence with exponent $\alpha = 2$. The error bar in the annotation refers to the 90% confidence interval in estimation of PSD.

Figure 5 displays the PSDs of the magnetic field along the perpendicular and parallel components as a function of frequency (f). The PSDs have been obtained using all our dataset regardless of the position of the satellite with respect to the Sun (dayside/nightside). These PSDs can be consequently considered as time averages on the selected polar hemisphere crossings. The spectral features are characterized by power-laws ($S(f) \propto f^{-\alpha}$) that span more than three decades of frequency ($0.005 \text{ Hz} < f < 4 \div 8 \text{ Hz}$) with spectral exponents α that lie in the range $\alpha \approx 2.0 \sim 2.5$. A clear difference in the energy content between parallel and perpendicular fluctuations is observed, while no relevant differences in the PSDs are observed between the two perpendicular directions inside the 90% confidence interval. Similar values have been found by Golovchanskaya *et al.* [2006] analyzing magnetic field observations by the DE2 satellite crossing the FAC regions in the polar ionosphere. Furthermore, as already discussed in Rother *et al.* [2007] the break near $4 \div 8 \text{ Hz}$ in the PSDs could be attributed to the fine structure of the FACs.

265 Figure 6 shows the same analysis, but this time separated into dayside and nightside
 266 crossings of FACs in the case of the two perpendicular components. A clear difference
 267 in the spectral law behavior is observed between dayside and nightside fluctuations; the
 268 dayside spectrum is less steep than the nightside one suggesting a less persistent nature of
 269 fluctuations.

270 Figures 5 and 6 show that the spectral exponents are larger than 2 in the analyzed
 271 range of frequencies. Similar results have been found by *Chaston et al.* [2008] analysing
 272 the magnetic and electric field fluctuations in the auroral oval using measurements on-
 273 board of the FAST satellite.



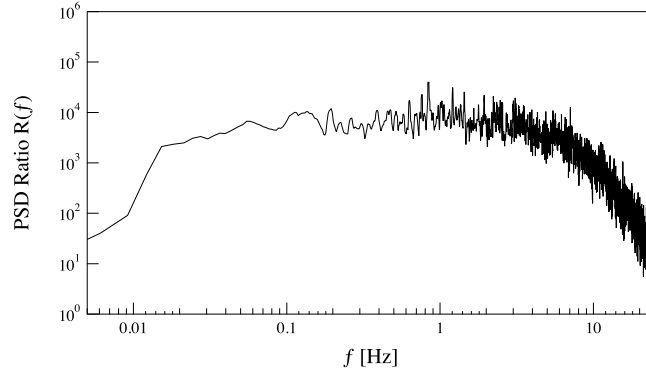
274 **Figure 6.** The average PSDs of the magnetic field fluctuations along the perpendicular components for the
 275 dayside and nightside crossings of FAC regions. PSDs show a slight different behavior with the frequency in
 276 terms of the observed spectral exponents ($\alpha \sim 2.1 \div 2.2$ in the dayside sector and $\alpha \sim 2.5 \div 2.6$ in the nightside
 277 sector - see dashed lines). The inset shows the ratio between the dayside and the nightside PSDs.

278 It is worth noting that the observed spectral exponents are larger than what is gener-
 279 ally expected for 3D MHD turbulence. Indeed, for ideal MHD turbulence the spectral
 280 exponent is expected in the range $\alpha \in (3/2, 5/3)$ as predicted by Iroshikov-Kraichnan
 281 and/or Kolmogorov theory of MHD and/or fluid turbulence [*Frisch*, 1995; *Biskamp*, 2003;
 282 *Bruno & Carbone*, 2016]. This discrepancy could be due to a strong anisotropy of the
 283 fluctuations as also suggested by the different energy content of fluctuations of the mag-
 284 netic field residual in the parallel and perpendicular directions to the main field. Indeed,
 285 as shown in Figure 5 the fluctuations in the parallel direction are strongly reduced in com-
 286 parison with perpendicular ones. This can be easily realized by analyzing the ratio, $R(f)$,
 287 between the perpendicular and parallel PSDs as a function of frequency (see Figure 7).
 288 The ratio $R(f)$, which is defined according to the following expression

$$R(f) = \frac{S_{\perp}^1(f) + S_{\perp}^2(f)}{2S_{\parallel}(f)}, \quad (1)$$

289 clearly shows that the energy spectra associated with the perpendicular components of the
 290 magnetic field fluctuations are characterized by values greater than those relative to the
 291 energy spectrum associated with the parallel component. This result suggests that turbu-
 292 lent fluctuations are restricted to a plane that is perpendicular to the main geomagnetic
 293 field local direction, thus indicating a possible reduction of the dimensionality of the tur-
 294 bulence, which in first approximation can be supposed to be quasi-bidimensional (2D).
 295 This means that the turbulent cascade occurs preferentially in the direction perpendicular
 296 to the main field. This view is also in agreement with the lack of plasma particle colli-

297 sions at the Swarm altitudes that implies the conductivity tensor off-diagonal elements to
 298 be essentially negligible, forcing the current to flow parallel to the main geomagnetic field
 299 direction.



300 **Figure 7.** Ratio, $R(f)$, between the normalized and time-averaged perpendicular and parallel energy spectra
 301 as a function of frequency.

302 The hypothesis of a 2D turbulence is also supported by the low values of the plasma
 303 β (the ratio of the plasma pressure to the magnetic pressure), $\beta \sim 10^{-3} - 10^{-4}$, which
 304 characterize these regions. In this configuration the magnetic fluctuations are, indeed,
 305 essentially confined to a plane perpendicular to the mean field, since field lines resist to
 306 bending in the parallel direction [Biskamp, 2003].

307 A possible explanation of the steeper PSDs observed in the case of magnetic field
 308 fluctuations in the FACs regions can be traced by simple dimensional arguments. In 3D
 309 fluid turbulence Kolmogorov's theory predicts a $-5/3$ spectral dependence for ho-
 310 mogeneous and isotropic turbulence. On the other hand, the Iroshnikov-Kraichnan the-
 311 ory for Alfvénic 3D turbulence predicts a power spectral density with a spectral exponent
 312 $\alpha = -3/2$. In these two cases the dimensionality of the turbulence in terms of number of
 313 free variables (degrees of freedom) is expected to be 3 and 4 for fluid and MHD turbu-
 314 lence, respectively. Now, the scaling properties of turbulent media are generally described
 315 in terms of q^{th} -order structure functions, S_q , i.e., the moments of the signal increments
 316 at different spatial scales, and their scaling with the different spatial scales. In particular,
 317 the corresponding q^{th} -order structure functions are expected to scale as $q/3$ and $q/4$ for
 318 homogeneous fluid and MHD turbulence, respectively, i.e.,

$$S_q(\delta r) = \langle |x(r + \delta r) - x(r)|^q \rangle \sim \delta r^{\gamma(q)}, \quad (2)$$

319 where x is the variable under investigation, δr is a spatial shift, and $\gamma(q) = q/3$ or $q/4$.
 320 In such a framework, the spectral exponent α is expected to be related to the second order
 321 structure exponent by the following relation (via the Wiener-Khinchine theorem),

$$\alpha = 1 + \gamma(2), \quad (3)$$

322 so that we get $\alpha = 5/3$ and $3/2$ for fluid and MHD turbulence, respectively. Taking
 323 into account that the fluctuations are essentially 2D in the FAC regions, if we suppose
 324 that these fluctuations are of Alfvénic nature (so that due to the Alfvénic correlation be-
 325 tween \vec{v} and \vec{b} fluctuations the degree of freedom reduces to 2), since they can be de-
 326 scribed in terms of Taylor force-free MHD equilibrium, we can expect that for 2D ho-
 327 mogeneous fluctuations, the q^{th} -order scaling exponent is $q/2$. Consequently, $\gamma(2) = 1$ and
 328 the spectral exponent is expected to be $\alpha = 2$. This result is not far from what is observed

329 in terms of average properties (see Figure 5). Clearly, intermittency corrections and/or
 330 anisotropic features in the plane perpendicular to the main magnetic field could modify
 331 the expected spectral exponent. In particular, the presence of anisotropy in the plane per-
 332 perpendicular to the main magnetic field could reduce the dimensionality of the fluctuation
 333 field, so that the effective dimension could be $D < 2$.

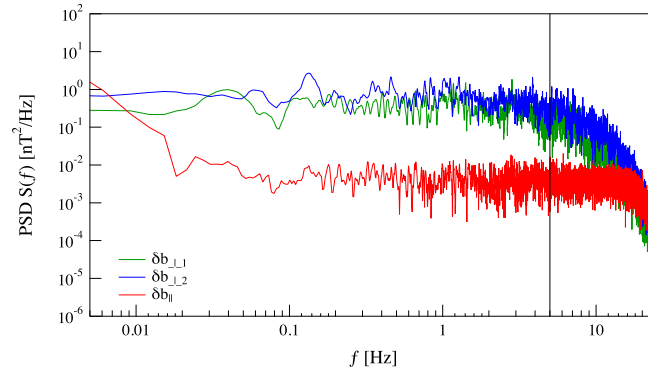
334 Moving to the analysis of the scaling features of magnetic field fluctuations we con-
 335 centrate our attention to the perpendicular components, which are expected to be strongly
 336 correlated with the structure of the FACs. Thus, we compute the so-called generalized
 337 structure functions of the magnetic field perpendicular components as a function of delay
 338 time τ , i.e.,

$$S_q(\tau) = \langle |b_i(t + \tau) - b_i(t)|^q \rangle, \quad (4)$$

339 where b_i is the i^{th} -component of the magnetic field residual, τ is the delay time and $\langle \dots \rangle$
 340 stands for a statistical average. For a scaling process, a power law behavior is expected,
 341 i.e.,

$$S_q(\tau) = \tau^{\xi(q)}, \quad (5)$$

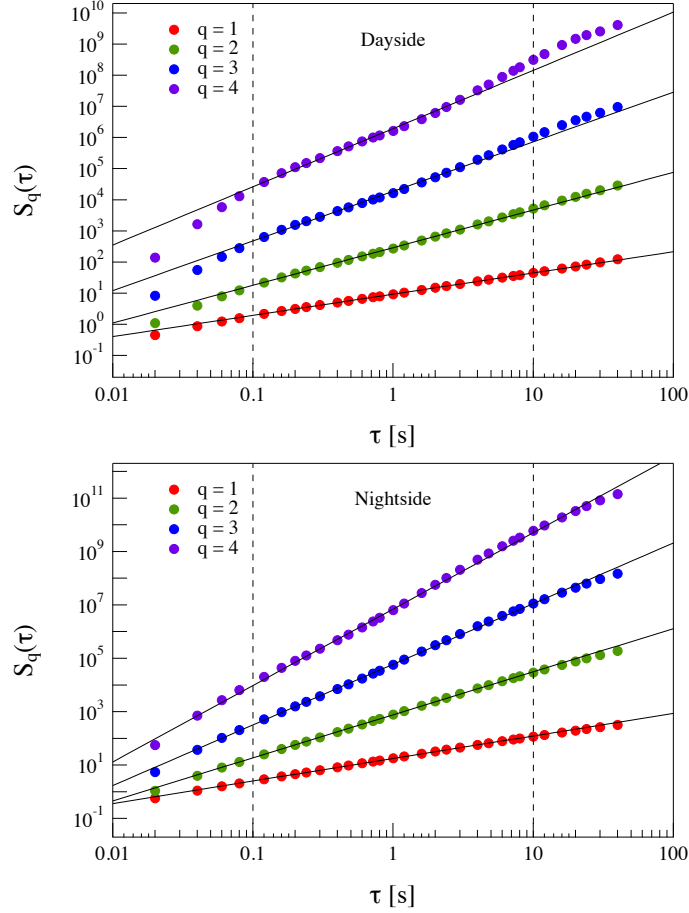
342 where $\xi(q)$ are the scaling exponents of the structure functions. In the case of simple frac-
 343 tal signals/structure these exponents are expected to be a linear function of the moment
 344 order q . Conversely, for more complex fractal signals/structures, such as inhomogeneous
 345 multifractals, the scaling exponents $\xi(q)$ show a departure from a linear dependence on
 346 the moment order q , being generally a convex function of q . This type of analysis can be
 347 applied in our study because, although the time series are non-stationary, they are charac-
 348 terized by stationary increments [Davis *et al.*, 1994; Mandelbrot *et al.*, 1997]. The PSDs
 349 of the time series relative to the increments of the magnetic field fluctuations along the
 350 parallel and perpendicular components, shown in Figure 8, are indeed characterized by
 351 quasi-flat spectral densities at frequencies below 5 - 10 Hz, which support the stationary
 352 character of the field increments [Davis *et al.*, 1994].



353 **Figure 8.** Power Spectral Density (PSD) of the increments of the magnetic field fluctuations along the
 354 three components: two perpendicular and one parallel to the main field. PSDs are expressed as a function of
 355 frequency and display a quasi-flat spectrum at frequencies less than 5 Hz.

356 Figure 9 shows the average q^{th} -order structure functions, $S_q(\tau)$, for different mo-
 357 ments q as a function of the time delay τ relatively to dayside/nightside crossings of FAC
 358 regions. In this case, we use all available data relative to the magnetic field fluctuations
 359 along the perpendicular directions to the main field. To compute the average structure

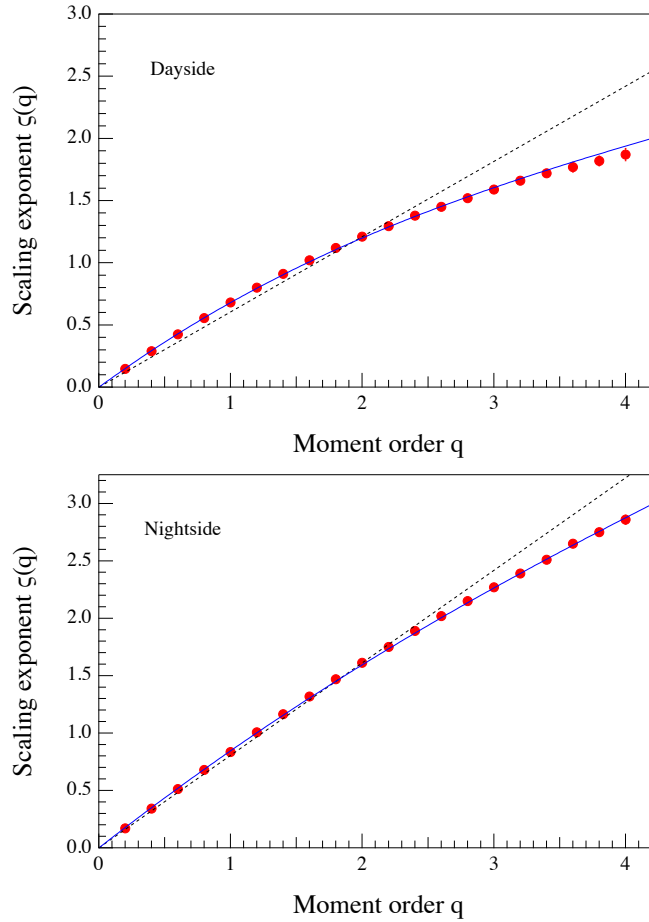
360 functions, the increments of each crossing are normalized by the standard deviation of
 361 the increments at the smallest timescale ($\tau = 0.02$ s). This operation is done in order
 362 to weight correctly the structure functions of the different FAC crossings when evaluat-
 363 ing the average scaling features. Power-law behavior of $S_q(\tau)$ is observed for all q 's in
 364 the range ~ 0.1 s $< \tau < 10$ s. The lower limit is related to the maximum frequency,
 365 $f_{max} \sim 1/2\tau \sim 5$ Hz, where a flat spectrum is observed. We stress that the range of scales,
 366 here investigated, is out of the PSD high-frequency spectral break, possibly related to in-
 367 tense kilometer-scale FACs [Rother *et al.*, 2007].



368 **Figure 9.** Average structure functions, $S_q(\tau)$, derived from the increments of the external magnetic field
 369 in the directions perpendicular to the main field, for moment q from 1 to 4 for dayside (upper panel) and
 370 nightside (lower panel) crossings. The two dashed lines delimit the region where the power law behavior is
 371 considered for estimating the scaling exponents.

372 The values of the scaling exponents $\xi(q)$ of the q^{th} -order structure functions, $S_q(\tau)$,
 373 estimated by using a least-square fitting in the range ~ 0.1 s $< \tau < 10$ s are reported
 374 in Figure 10 for moment $q \in [0, 4]$. Here, two different panels are presented. In the up-
 375 per panel we show the scaling exponents, $\xi(q)$, relative to the dayside crossings of FACs,
 376 while in the lower panel the same quantities for nightside crossings of FACs are shown.

381 For both dayside and nightside crossings of FACs regions the magnetic field incre-
 382 ments show anomalous scaling properties. Indeed, the values of the scaling exponents
 383 $\xi(q)$ are not characterized by a linear dependence on q , and that marks the occurrence



377 **Figure 10.** Behavior of the scaling exponents $\xi(q)$ relative to the structure functions of the increments of
 378 the magnetic field residuals in the plane perpendicular to the main field recorded during the dayside (upper
 379 panel) and nightside (lower panel) crossings of FACs. The dashed lines refer to linear scaling (monofractal
 380 behavior) while blue curves are related to the generalized P-model.

384 of anomalous scaling features, i.e., a multifractal structure of the magnetic field fluctu-
 385 ations. This is the evidence for the occurrence of intermittency. Intermittency is a very
 386 peculiar feature of fluid and magnetohydrodynamic turbulence [Frisch, 1995; Biskamp,
 387 2003; Bruno & Carbone, 2016]. This property is the consequence of the local nature of
 388 the ideal Richardson's cascade due to its stochastic nature (Landau's remark on the Kol-
 389 mogorov/Obukhov K41 theory of turbulence [Kolmogorov, 1962; Frisch, 1995]) so that
 390 the resulting dissipation field is no longer homogeneous in terms of scaling its features
 391 [Frisch, 1995]. In other words, intermittency is a manifestation of a multifractal structure
 392 of the dissipation field, i.e., the dissipation is sporadically localized in the space (and also
 393 in time).

394 To better characterize the deviation from linearity of the observed scaling expo-
 395 nents $\xi(q)$, we compare it with the expected behavior predicted by a generalized two-scale
 396 Cantor set or P-model. In the case of 3D fully-developed fluid and MHD turbulence the
 397 anomalous scaling of the exponent of the q^{th} -order structure function as a function of
 398 the moment order q can be modeled by the P-model [Meneveau and Sreenivasan, 1987],
 399 which predicts

$$\xi(q) = 1 - \log_2 \left(p^{\frac{q}{3}} + (1-p)^{\frac{q}{3}} \right) \quad (6)$$

400 and

$$\xi(q) = 1 - \log_2 \left(p^{\frac{q}{4}} + (1-p)^{\frac{q}{4}} \right) \quad (7)$$

401 for the fluid and MHD turbulence, respectively. In our case the dimensionality of the ob-
 402 served turbulent fluctuations is neither 3 nor 4, so we can try to fit the observed behavior
 403 of $\xi(q)$ by a generalization of the last two expressions, i.e.,

$$\xi(q) = 1 - \log_2 \left(p^{\frac{q}{d}} + (1-p)^{\frac{q}{d}} \right), \quad (8)$$

404 where the parameter d is representative of an effective dimension of the fluctuation field.
 405 Figure 10 reports the fit of the trend $\xi(q)$ using the generalized P-model (see Eq. 8). The
 406 fits are excellent for both dayside and nightside sectors. The fitting parameters are $p =$
 407 $[0.76 \pm 0.01]$ and $d = [1.58 \pm 0.01]$ for dayside FAC crossings, and $p = [0.66 \pm 0.01]$ and
 408 $d = [1.20 \pm 0.01]$ for nightside FAC crossings, respectively. In both cases the parameter $p \neq$
 409 0.5 indicating that the fluctuation field is not homogeneous (i.e., we are in the presence
 410 of an inhomogeneous dissipation pattern). The higher value of the p parameter for the
 411 dayside FAC sector supports the higher degree of intermittency of fluctuations/increments
 412 in that region. Furthermore, the observed effective dimension, d , is higher in the dayside
 413 than in the nightside suggesting a different degree of correlation of the fluctuations in the
 414 perpendicular direction to the main magnetic field. We note that the effective dimensions
 415 agree very well with the observed spectral exponents as $\alpha = 2/d + 1$ ($\alpha \sim 2.2$ and ~ 2.6
 416 for dayside and nightside sectors, respectively).

417 Thus, the magnetic field fluctuations in the FAC regions are characterized by an inter-
 418 mittent turbulence that tends to localize large fluctuations (i.e., energy) in small spatial
 419 regions, or “hot spots”. Furthermore, the obtained results provide the evidence that this
 420 intermittent character (anomalous scaling) is higher in the dayside sector than in the night-
 421 side one.

422 4 Discussion and Conclusions

423 We have investigated the nature of the magnetic field fluctuations in the topside F-
 424 region of the ionosphere using the high-resolution (50 Hz) magnetic field measurements
 425 recorded by the Swarm ESA’s Earth Observation mission. In detail, we have carefully
 426 examined the small-scale low frequency magnetic field fluctuations in the high-latitude
 427 ionospheric regions, associated with the field-aligned currents. For this reason, we have
 428 analyzed the components of the magnetic field residual of external origin with directions
 429 parallel and perpendicular to the main field and evaluated the spectral and scaling features
 430 of these small-scale magnetic field fluctuations recorded in the FAC regions.

431 From our study it emerges that:

- 432 • as expected the magnetic field fluctuations/increments are strongly anisotropic (see
 433 Figure 5) and essentially confined to the plane perpendicular to the main field sug-
 434 gesting that the fluctuations are essentially 2D;
- 435 • the spatio-temporal magnetic field fluctuations in the perpendicular plane show
 436 scale invariance over nearly two and half orders of magnitude (see Figure 9), which
 437 is one of the properties of observed turbulence;
- 438 • the obtained scale invariance is anomalous (see Figure 10), suggesting the occur-
 439 rence of intermittency, i.e., large amplitude fluctuations that are strongly localized
 440 in the space and time;

- the intermittent character (anomalous scaling) exhibits a dependence on MLT sectors displaying a significant increase in the dayside (see Figure 10).

These results support the idea of the occurrence of intermittent turbulence in the regions of FACs. The observed spectral character of a 2D turbulence resembles the numerical results of 2D ideal compressible MHD simulations by *Chang et al.* [2004], that found the formation of a spectral domain $S(k) \sim k^{-2}$. Clearly, the similarity between our results and *Chang et al.* [2004] 2D MHD simulations requires the assumption that Taylor's hypothesis is valid, i.e., that the frequency f , measured in the spacecraft reference system, is related to the wave number k by the simple relationship $2\pi f \sim v_{sp}k$, where v_{sp} is the spacecraft speed (~ 8 km/s). This hypothesis has been shown to be reasonable for the crossing of field-aligned current regions and in other works dealing with observations of turbulence in auroral regions [see e.g. *Chaston et al.*, 2008, and references therein]. Actually, to be more precise, this hypothesis is different from the Taylor hypothesis argument in the solar wind, where the solar wind moves much faster than that of the spacecraft. Indeed, according to 2D MHD calculations of the inertial Alfvénic fluid equations, the interacting coherent structures form nearly 2-d static potential structures, and thus, as a satellite moves across these nearly static structures they exhibit low frequency fluctuations due to Doppler shifts. Furthermore, the range of investigated timescales (from 0.1 s up to 10 s) deals with time intervals where it can be reasonably assumed that the structures are mainly frozen, as also reported in other papers [e.g. *Gjerloev et al.*, 2011; *De Michelis et al.*, 2017]. Indeed, it has been clearly shown that in the dayside/nightside sectors the FAC structures are nearly stable up to 60/160s, respectively. In other words, we assume that the structures do not evolve in time during the spacecraft crossing at the investigated range of scales. This assumption is supported by the previous discussion on the link between the Doppler-shift and fluctuation in the low-frequency range reported in Section 3 [see, also *Kintner and Seyler*, 1985]. Furthermore, we can expect that the evolution time for structures in a turbulent medium could be longer than that of the typical nonlinear time associated with the corresponding wave-number. This is also confirmed by looking at the PSD of field increments (see Figure 8) which displays a quasi-flat behaviour in the range of the investigated timescales, supporting a quasi-stationarity condition.

Due to the strong magnetic field in the polar regions and to its quasi-uniform and unidirectional character, the variations/perturbations along the main geomagnetic field direction are damped by the plasma dynamics in the parallel direction [*Biskamp*, 2003]. In this picture the field is essentially potential and a reasonable approximation to describe the emerging scenario is the *Reduced Magneto-Hydro-Dynamics* (RMHD) [refer to *Biskamp*, 2003]. The magnetic field fluctuations, although small, dominate in the perpendicular directions with respect to the mean magnetic field B_0 , and thus they can be described by a flux function, $\psi(x, y)$, i.e.,

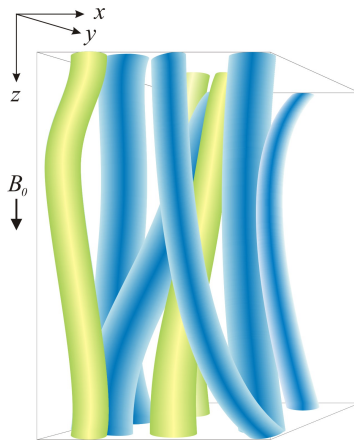
$$\mathbf{B} = \mathbf{e}_z \times \nabla\psi + B_0\mathbf{e}_z \rightarrow \mathbf{B} = (\delta B_x, \delta B_y, B_0), \quad (9)$$

where the z-direction is aligned to the mean field and $B_0 \equiv B_z$ is assumed to be constant and large with respect to the perpendicular field, $B_\perp/B_z \ll 1$. Here the flux function ψ , which is associated with the poloidal field, is essentially the axial component of the vector potential A_z , i.e., $\psi = -A_z$, and represents the magnetic field flux. The nearly force-free condition for the mean field and the current density conservation, $\nabla \cdot \mathbf{J} \sim 0$, imply that $\mathbf{B} \cdot \nabla J_z \sim 0$ [see *Chang et al.*, 2004], i.e.,

$$B_0 \frac{\partial J_z}{\partial z} = - \left(\frac{\partial \psi}{\partial y} \frac{\partial}{\partial x} - \frac{\partial \psi}{\partial x} \frac{\partial}{\partial y} \right) J_z + \dots, \quad (10)$$

where the ellipsis indicates the possible occurrence of other non-ideal terms which are associated with some modifying effects. Neglecting the ellipsis and including the Ampère's law a simple solution of Eq. (10) for the axial current J_z and the flux function ψ

488 is the class of circularly cylindrical field-aligned flux tubes (see Figure 11), which can be
 489 considered as coherent structures [Wu and Chang, 2000, 2001; Chang *et al.*, 2004]. The
 490 dynamics of these coherent structures can strongly affect the local plasma and magnetic
 491 field topologies, and can be a possible source of the observed intermittent turbulent fluctu-
 492 ations. On the other hand, the formation of multi-scale coherent field-aligned structures
 493 implies the generation of a very complex pattern of the current density J_z , which may re-
 494 sult to be strongly inhomogeneous in the direction perpendicular to the mean magnetic
 495 field. We note how this scenario is compatible with approximate force-free equilibrium,
 496 $\nabla \times \mathbf{B} \sim \theta \mathbf{B}$ (here θ is a constant), which is a minimal free-energy condition accord-
 497 ing to the Woltjer Theorem. In this framework, the potential structures should explain the
 498 observed nearly field-aligned interacting current filaments that in turn produce the cor-
 499 responding low frequency magnetic fluctuations. Thus, low frequency satellite magnetic
 500 field measurements provide nearly 2d spatial fluctuating signatures [see e.g., Tam *et al.*,
 501 2010]. However, due to the sporadic interactions among the filamentary structures gener-
 502 ated by the non-ideal dissipative effects and the complexity phenomenon of coarse-grained
 503 dissipation [Chang *et al.*, 2004], entrained within these nearly stationary spatial structures
 504 there are probably small fractions of temporal fluctuations, some random/stochastic and
 505 some with electrostatic/electromagnetic ion cyclotron or inertial/kinetic Alfvén wave char-
 506 acteristics.



507 **Figure 11.** A sketch of coherent field-aligned flux tubes in a quasi force-free equilibrium. The current is
 508 aligned along magnetic structures. The colors refer to different directions of the field-aligned currents.

509 This scenario can pave the way to a better understanding of the nature of the small-
 510 scale field-aligned currents observed throughout the auroral oval [Lühr *et al.*, 1994; Stasiewicz
 511 and Potemra, 1998; Neubert and Christiansen, 2003] which, as suggested by the presence
 512 of 2D intermittent turbulence of the magnetic field fluctuations associated with these cur-
 513 rents, could be filamentary and inhomogeneous. Thus, our results seem to support the pre-
 514 vious hypothesis according to which the field-aligned currents on small scales are ran-
 515 domly oriented thus reflecting a filamentary structure [Neubert and Christiansen, 2003].

516 However, all this picture is strongly dynamic, so that the current field pattern and
 517 the associated magnetic field structures are continuously evolving. This is the origin of the
 518 observed intermittent turbulence.

519 Really, we cannot exclude that there are also other possible scenarios compatible
 520 with what found, such as the occurrence of electrostatic turbulent fluctuations in dynami-
 521 cal equilibrium with $\mathbf{E} \times \mathbf{B}$ drift velocity shear (as it occurs in tokamak edge turbulence),
 522 which exhibits strong intermittency and formation of coherent structures, playing a rele-

523 vant role in driving energy losses [see e.g., *Tam et al.*, 2005; *Golovchanskaya et al.*, 2006;
524 *Lepreti et al.*, 2009, and references therein].

525 The validation of the most appropriate scenario requires the investigation of other
526 physical quantities and multifractal properties such as those described in the monograph
527 by *Chang* [2015] and will be the topic of a future work.

528 Acknowledgments

529 The results presented rely on data collected by one of the three satellites of the
530 Swarm constellation. We thank the European Space Agency (ESA) that supports the Swarm
531 mission. Swarm data can be accessed online at <http://earth.esa.int/swarm>. The authors
532 kindly acknowledge V. Papitashvili and J. King at the National Space Science Data Center
533 of the Goddard Space Flight Center for the use permission of 1 min OMNI data and the
534 NASA CDAWeb team for making these data available at <https://cdaweb.gsfc.nasa.gov/index.html/>.
535 This work is supported by ESA under contract ESA Contract No. 4000125663/18/I-NB
536 (INTENS).

537 References

- 538 Anderson, B. J., Ohtani, S.-I., Korth, H., and Ukhorskiy, A. (2005), Storm time dawn-
539 dusk asymmetry of the large-scale Birkeland currents, *J. Geophys. Res.*, 110, A12220,
540 doi:10.1029/2005JA011246.
- 541 Anderson, B. J., Korth, H., Waters, C. L., Green, D. L., and Stauning, P. (2008), Statistical
542 Birkeland current distributions from magnetic field observations by the Iridium constel-
543 lation, *Ann. Geophys.*, 26, 671-687, doi:10.5194/angeo-26-671-2008.
- 544 Angelopoulos, V., Mukai, T., and Kokubun, S. (1999), Evidence for intermittency in
545 Earth's plasma sheet and implications for self-organized criticality, *Phys. Plasmas*, 6,
546 4161.
- 547 Birkeland K. (1908), *The Norwegian Aurora Polaris Expedition, 1902-1903*, pp. 998, H.
548 Aschehoug & Co., Christiania.
- 549 Biskamp D., and Schwarz, H. (2001), On two-dimensional magnetohydrodynamic turbu-
550 lence, *Phys. Plasmas*, 8, 3282-3292.
- 551 Biskamp D. (2003), *Magnetohydrodynamic turbulence*, Cambridge University Press.
- 552 Booker, H.G. (1956), Turbulence in the ionosphere with applications to meteor-trails,
553 radio-star scintillation, auroral radar echoes, and other phenomena, *J. Geophys. Res.*,
554 61 (4), 673.
- 555 Borovsky J.E., Elphic, R.C., Funsten, H.O., and Thomsen, M.F. (1997), The Earth's
556 plasma sheet as a laboratory for flow turbulence in high- β MHD, *J. Plasm. Phys.*, 57,
557 1-34.
- 558 Bruno R., and Carbone, V. (2016), *Turbulence in the Solar Wind*, *Lect. Notes Phys.*, 928,
559 Springer, doi:10.1007/978-3-319-43440-7.
- 560 Chang T., Tam, S., Wu, C.-C., and Consolini, G. (2003), Complexity, Forced and/or Self-
561 Organized Criticality, and topological phase transitions in space plasmas, *Space Sci.*
562 *Rev.*, 107, 425-445.
- 563 Chang T., S. Tam, and C.-C. Wu (2004), Complexity induced anisotropic bimodal inter-
564 mittent turbulence in space plasmas, *Phys. Plasmas*, 11, 1287-1299.
- 565 Chang T., (2015), *An Introduction to Space Plasma Complexity*, Cambridge University
566 Press, New York, NY.
- 567 Chaston C.C., et al. (2008) The turbulent Alfvénic aurora, *Phys. Rev. Lett.*, 100, 175003.
- 568 Cheng, Z. W., Shi, J. K., Dunlop, M., and Liu, Z. X. (2013): Influences of the interplane-
569 tary magnetic field clock angle and cone angle on the field-aligned currents in the mag-
570 netotail, *Geophys. Res. Lett.*, 40, 5355-5359, doi:10.1002/2013GL056737.

- 571 Chisham, G., et al. (2007): A decade of the Super Dual Auroral Radar Network (Super-
572 DARN): scientific achievements, new techniques and future directions, *Surv. Geophys.*,
573 28, 33-109, doi:10.1007/s10712-007-9017-8.
- 574 Christiansen, F., Papitashvili, V. O., and Neubert, T. (2002), Seasonal variations of high
575 latitude field-aligned currents systems inferred from Oersted and Magsat observations, *J.*
576 *Geophys. Res.*, 107, 1029, doi:10.1029/2001JA900104.
- 577 Cummings W. D., and Dessler, A. J. (1967), Field-aligned currents in the magnetosphere,
578 *Journal of Geophysical Research*, 72, 1007-1013, doi: 10.1029/JZ072i003p01007.
- 579 Dagg, M. (1957), The origin of the ionospheric irregularities responsible for radio-star
580 scintillations and spread-F-II: Turbulent motion in the dynamo region, *J. Atmospheric*
581 *Terrestrial Phys.*, 11, 139.
- 582 Davis, A., Marshak, A., Wiscombe, W., and Cahalan, R. (1994), Multifractal characteriza-
583 tions of nonstationarity and intermittency in geophysical fields: Observed, retrieved, or
584 simulated, *Journal of Geophysical Research*, 99, 8055-8072.
- 585 De Michelis, P., Consolini, G., and Tozzi, R. (2015), Magnetic field fluctuation fea-
586 tures at Swarm's altitude: A fractal approach, *Geophys. Res. Lett.*, 42, 3100-3105.
587 <https://doi.org/10.1002/2015GL063603>.
- 588 De Michelis, P., Consolini, G., Tozzi, R., and Marcucci, M. F. (2017), Scaling
589 features of high-latitude geomagnetic field fluctuations at Swarm altitude: Im-
590 pact of IMF orientation, *J. Geophys. Res.: Space Physics*, 122, 10,548-10,562.
591 <https://doi.org/10.1002/2017JA024156>.
- 592 De Michelis, P., Consolini, G., Tozzi, R., Giannattasio, F., Quattrociochi, V. and Coco,
593 I. (2019), Features of magnetic field fluctuations in the ionosphere at Swarm altitude,
594 *Annals Geophys.*, 62, GM499. <https://doi.org/10.4401/ag.7789>.
- 595 Finlay, C. C. (2015), DTU candidate field models for IGRF-12 and the CHAOS-5 geo-
596 magnetic field model, *Earth, Planets and Space* 67, 114.
- 597 Friis-Christensen, E., Lühr, H., and Hulot, G. (2006), Swarm: a constellation to study the
598 earth's magnetic field, *Earth Planets Space*, 58, 351.
- 599 Frisch U. (1995), *Turbulence: the legacy of A.N. Kolmogorov*, Cambridge University Press.
- 600 Gjerloev, J. W., Ohtani, S., Iijima, T., Anderson, B., Slavin, J., and Le, G. (2011), Charac-
601 teristics of the terrestrial field-aligned current system, *Ann. Geophys.*, 29, 1713-1729.
- 602 Golovchanskaya, I. V., Ostapenko, A. A., and Kozelov, B. V. (2006), Relation-
603 ship between the high-latitude electric and magnetic turbulence and the Birke-
604 land field-aligned currents. *Journal of Geophysical Research*, 111, A12301.
605 <https://doi.org/10.1029/2006JA011835>.
- 606 Iijima, T., and Potemra, T. A. (1976), Field-aligned currents in the dayside cusp observed
607 by Triad, *J. Geophys. Res.*, 81(34), 5971-5979, doi:10.1029/JA081i034p05971.
- 608 Iijima, T., and Potemra, T. A. (1978), Large-scale characteristics of field-aligned
609 currents associated with substorms, *J. Geophys. Res.*, 83(A2), 599-615,
610 doi:10.1029/JA083iA02p00599.
- 611 Iijima, T. (1984), Field-aligned currents during northward IMF, in *Geophysical Monograph*
612 *Series: Magnetospheric currents*, Vol. 28 doi: 10.1029/GM028p0115.
- 613 Iijima T. and Shibaji, T. (1987), Global characteristics of northward IMF-associated (NBZ)
614 field-aligned currents, *J. Geophys. Res.*, 92, 2408.
- 615 Keller, K.A., Lysak, R.L., and Song, Y. (1999), A three-dimensional simulation of the
616 Kelvin-Helmholtz instability, in *Magnetospheric Current Systems*, S. Ohtani, R. Fujii,
617 M. Hesse and R. L. Lysak Eds., AGU Geophysical Monograph 118.
- 618 Kintner, P.M., and Seyler, C.E. (1985), The status of observations and theory of high lati-
619 tude ionospheric and magnetospheric plasma turbulence, *Space Sci. Rev.*, 41, 91.
- 620 Knudsen, D. J., Burchill, J. K., Buchert, S. C., Eriksson, A. I., Gill, R., Wahlund, J.-
621 E. , L. Ahlen, Smith, M., and Moffat, B. (2017), Thermal ion imagers and Langmuir
622 probes in the Swarm electric field instruments, *J. Geophys. Res. Space Physics*, 122.
623 <https://doi.org/10.1002/2016JA022571>.

- 624 Kolmogorov, A. N. (1941a), Energy dissipation in locally isotropic turbulence. Doklady
625 Akad. Nauk SSSR , 32 (1), 19?21.
- 626 Kolmogorov, A. N. (1941b), Local structure of turbulence in an incompressible fluid at
627 very high Reynolds numbers. Dokl. Akad. Nauk SSSR, 30, 301.
- 628 Kolmogorov, A. N. (1962), A refinement of previous hypotheses concerning the local
629 structure of turbulence in a viscous incompressible fluid at high Reynolds number. J.
630 Fluid Mech. 13, 82.
- 631 Korth, H., Anderson, B. J., and Waters, C. L. (2010), Statistical analysis of the depen-
632 dence of large-scale Birkeland currents on solar wind parameters, *Ann. Geophys.*, 28,
633 515-530, doi:10.5194/angeo-28-515-2010.
- 634 Lepreti F., et al. (2009), Yaglom law for electrostatic turbulence in laboratory magnetized
635 plasmas, *Europhys. Lett.*, 86, 25001, doi: 10.1209/0295-5075/86/25001.
- 636 Lühr H., Warnecke, J., Zanetti, L. J., Lundquist, P. A., and Hughes, T. J. (1994), Fine
637 structure of field-aligned current sheets deduced from spacecraft and ground-based ob-
638 servations: Initial Freja results, *Geophys. Res. Lett.*, 21, 1883.
- 639 Lühr H., Huang, T., Wing, S., Kervalishvili, G., Rauberg, J. and Korth, H. (2016), Fila-
640 mentary field-aligned currents at the polar cap region during northward interplanetary
641 magnetic field derived with the Swarm constellation, *Ann. Geophys.*, 34, 901-915, doi:
642 10.5194/angeo-34-901-2016.
- 643 Lui A.T.Y., et al. (1998), Plasma and magnetic flux transport associated with auroral
644 breakups, *Geophys. Res. Lett.*, 25, 4059.
- 645 Mandelbrot, B. B., Fisher, A. J., and Calvet, L. E. (1997), A Multifractal Model of Assets
646 Returns. Cowles Foundation discussion paper no. 1164.
- 647 Meneveau C., and Sreenivasan, K.R. (1987), Simple multifractal cascade for fully devel-
648 oped turbulence, *Phys. Rev. Lett.*, 59, 1424-1427.
- 649 Neubert, T., and Christiansen, F. (2003), Small-scale, field-aligned currents at the top-side
650 ionosphere, *Geophys. Res. Lett.*, 30(19) doi:10.1029/2003GL017808.
- 651 Olsen, N. (1996), A new tool for determining ionospheric currents from magnetic satellite
652 data, *Geophys. Res. Lett.* , 23 , 3635, <http://doi.org/10.1029/96GL02896>.
- 653 Papitashvili V. O., Christiansen, F., and Neubert, T. (2001), Field-aligned currents during
654 IMF 0, *Geophys. Res. Lett.*, 28, 3055-3058.
- 655 Papitashvili, V. O. and Rich, F. J. (2002), High-latitude ionospheric convection models de-
656 rived from Defense Meteorological Satellite Program ion drift observations and param-
657 eterized by the interplanetary magnetic field strength and direction, *J. Geophys. Res.*,
658 107, 1198, doi:10.1029/2001JA000264.
- 659 Pokhotelov, O.A., Pilipenko, V.A., Fedorov, E.N., Stenflo, L., and Shukla, P.K. (1994),
660 Induced electromagnetic turbulence in the ionosphere and the magnetosphere, *Physica*
661 *Scripta*, 50, 600.
- 662 Ritter P., Lühr, H., and Rauberg, J. (2013), Determining field-aligned currents
663 with the Swarm constellation mission, *Earth Planets Space*, 65, 1285-1294, doi:
664 10.5047/eps.2013.09.006.
- 665 Rother, M., Schlegel, K., and Lühr, H. (2007), CHAMP observation of intense kilometer-
666 scale field-aligned currents, evidence for an ionospheric Alfvén resonator, *Ann. Geo-*
667 *phys.*, 25, 16031615, doi: 10.5194/angeo-25-1603-2007.
- 668 Spicher, A., Miloch, W.J., Clausen, L.B.N. and Moen, J. I. (2015), Plasma turbulence and
669 coherent structures in the polar cap observed by the ICI-2 sounding rocket, *J. Geophys.*
670 *Res. Space Physics*, 120, 10,959-10,978, doi:10.1002/2015JA021634.
- 671 Sofko, G.J., Greenwald, R., and Bristow, W. (1995): Direct determination of large-scale
672 magnetospheric field-aligned currents with SuperDARN, *Geophys. Res. Lett.*, 22, 2041-
673 2044.
- 674 Stasiewicz, K., and Potemra, T. (1998), Multiscale current structures observed by Freja, *J.*
675 *Geophys. Res.*, 103, 4315.
- 676 Tam Sunny W. Y., Chang, T., Kintner, P. M., and Klatt, E. (2005), Intermittency analy-
677 ses on the SIERRA measurements of the electric field fluctuations in the auroral zone,

- 678 Geophys. Res. Lett., 32, CiteID L05109.
- 679 Tam Sunny W. Y., Chang, T., Kintner, P. M., and Klatt, E. (2010), ROMA (Rank-Ordered
680 Multifractal Analysis) for intermittent fluctuations with global crossover behavior, *Phys.*
681 *Rev. E*, 81, 036414.
- 682 Wu, C. C. and Chang, T. (2000), 2D MHD simulation of the emergence and merging of
683 coherent structures, *Geophys. Res. Lett.*, 27, 863.
- 684 Wu, C. C. and Chang, T. (2001), Further study of the dynamics of two-dimensional MHD
685 coherent structures large scale simulation, *J. Atmos. Sol. Terr. Phys.*, 63, 1447.
- 686 Zmuda A. J., Martin, J.H., and Heuring, F.T. (1966), Transverse hydromagnetic distur-
687 bances at 1100 km in the auroral region, *J. Geophys. Res.*, 71, 5033-5045.